Polarization of the A-Band Emission from RbCl:Pb²⁺

Jun-Gill Kang

Department of Chemistry, Chungnam National University, Chungnam 300-31. *Received January 22, 1986*

The angular dependence of polarization of the A-band emission from RbCl:Pb²⁺ is measured at 13.4 K to determine the symmetry axes of the Pb^{2+}-v_c^- dipoles. The results indicate that these centers posess tetragonal symmetry. This implies that v_c^- is situated in the next-nearest-neighbor (nnn) position to the Pb^{2+} ion. The polarization ratio of the A-band emission measured at various temperatures is found to be independent of the temperature. The temperature independence of polarization confirms that, for the Pb^{2+} ion, the Jahn-Teller effect reduced by strong spin-orbit interaction does not give rise to thermal depolarization.

Introduction

The first detailed investigation of the luminescence polarization of diatomic molecules, complex molecules and also of polarization phenomena in crystals was undertaken by Feofilov[1]. Polarization phenomena in crystals are particularly useful in revealing the structure and the presence of symmetry axes associated with anisotropic luminescent centers. The polarization of the A-band emission from Tl^+-like ions (Ga^+, In^+, Sn^{2+}) in alkali halide single crystals has been extensively studied[2-6]. At liquid helium temperature, polarized luminescence was observed in most of alkali halide phosphors and with increasing temperature the polarization was strongly reduced. A quantitative explanation for the temperature dependence of polarization was given in terms of the Jahn-Teller interaction with the tetragonal $E_g(Q_2, Q_3)$ vibronic modes. The reduction of the polarization results from the relaxation inside the Jahn-Teller wells and transitions between the orthorhombic wells due to the perturbation of the Jahn-Teller tetragonal distortion by the trigonal T_{1g} (Q_4, Q_5, Q_6) vibronic modes. Previously we reported the polarized emission from KX:Pb^{2+} (X = Cl, Br, I)[7,8]. The luminescent centers have some characteristic symmetry axes, depending on the location of the charge compensating cation vacancy (CCV, v_c^-), *i.e.*, the nearest-neighbor (nn) and/or next-nearest-neighbor (nnn) positions to Pb^{2+} ion. The degree of polarization of the principal A-band emission from KCl:Pb^{2+} and KBr:Pb^{2+} is nearly independent of temperature, while that from KI:Pb^{2+} decreases with increasing temperature up to 50 K becoming constant above 50 K. The temperature dependence of polarization was treated in terms of the energy-level scheme for Pb^{2+} color center in the crystal field.

We previously reported the A-band emission from RbCl:Pb^{2+} and presented the first assignment of the emission in terms of the adiabatic potential energy surface (APES) of the $^3T_{1u}^*$ state[9]. At low temperature, a strong emission band is observed at low energy side (3.5 eV), which is referred to as A_X, with a weak band at high energy side (3.85 eV) referred to as A_T^*. In the present work, the angular dependence of the polarization ratio of the A-band emission from RbCl:Pb^{2+} is investigated to reveal the symmetry of the Pb^{2+}-v_c^- dipoles. The results are used to suggest a mechanism for nonradiative processes in relaxed excited states (RES's).

Experimental

Measurements were performed of both the poarization spectra (*i.e.*, the degree of polarization of the A-band emission as a function of the photon energy of the exciting light), and the diagram of the polarization ratio (*i.e.*, the dependence of the emission polarization on the orientational angle of the polarized excitation beam with respect to the crystal axes). The polarization measurements were almost the same as those used in previous works[8,9]. A glan-air prism polarizer and an analyzer were used. The analyzer consisted of a polaroid HNP'B sheet polarizer without the quarter wave plate, since the plate made of plastic material did not transmit light below 400 nm (and hence absorbed light emitted from RbCl:Pb^{2+}). In this case, the raw data were corrected taking into account the response of the monochromator to the polarized emission. All polarization measurements were performed with perpendicular geometry because of experimental difficulties in the elimination of stray light. In Figure 1, the orientation of the polarizer in the excitation beam with respect to the z axis is denoted by an angle α. The corresponding angle for the analyzer is denoted by β. For each value of α, two emission intensities were recorded: one with the analyzer set at $\beta = \alpha$ (referred to as $I_{\parallel}(\alpha)$) and one perpendicular, *i.e.*, $\beta = \alpha + \pi/2$ (referred to as $I_{\perp}(\alpha)$). The polarization ratio is defined as[10] $P(\alpha) = \{I_{\parallel}(\alpha) - I_{\perp}(\alpha)\}/\{I_{\parallel}(\alpha) + I_{\perp}(\alpha)\}$ and in this paper, the degree of polarization is referred to as the polarization ratio when $\alpha = 0$ or 180°.

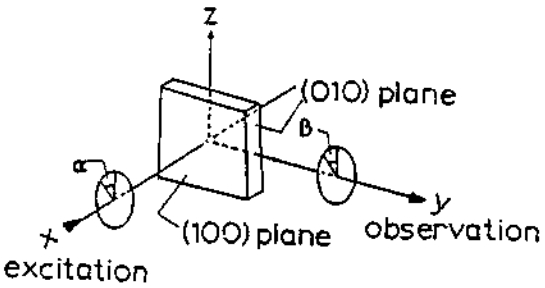

Figure 1. Block diagram of perpendicular arrangement for polarization measurements. α: angle of polarizer, β: angle of analyzer.

Experimental Results

The polarized emission spectra of RbCl:Pb^{2+} excited at 270 nm ($\alpha = 0°$, T = 13.4 K) were measured. As shown in Figure 2, both of the A_X (peaked at 354 nm) and the A_T^* (peaked at 322 nm) are polarized with positive values of the degree of polarization. Also, the excitation dependence of the degree of polarization of the two emission bands was measured at

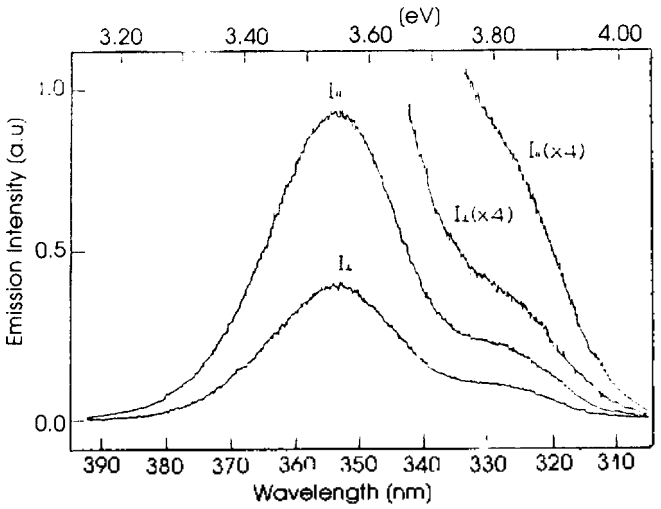

Figure 2. Uncorrected emission spectra of RbCl:Pb^{2+} excited at 270 nm polarized at $\alpha = 0°$ and $\beta = 0°$ for $I_{\parallel}$ and $\beta = 90°$ for $I_{\perp}$ (T = 13.4 K).

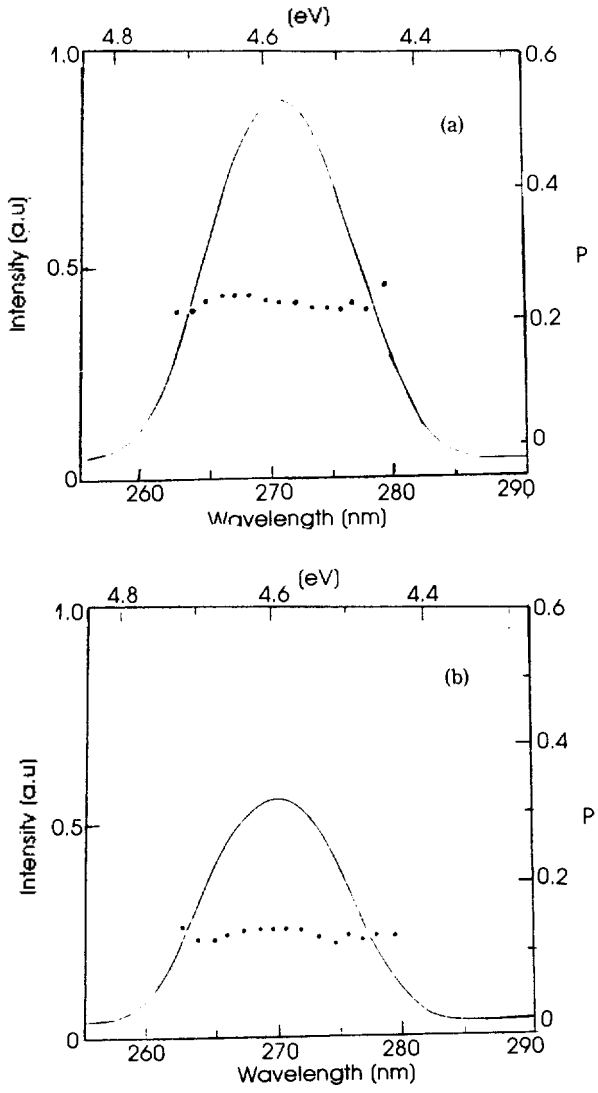

Figure 3. Polarization spectra (T = 13.4 K) of: (a) the 354 nm and (b) the 322 nm emissions from RbCl:Pb^{2+}. Solid line and solid circule indicate the excitation spectrum and the degree of polarization, respectively.

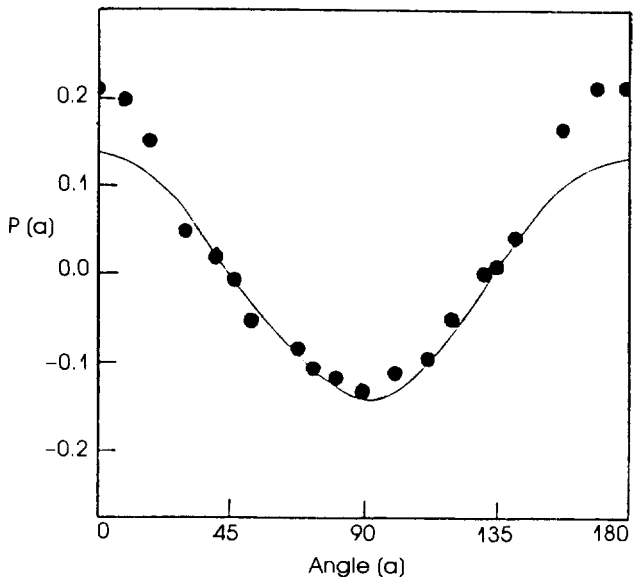

Figure 4. Diagram of the polarization ratio of the 354 nm emission from RbCl:Pb^{2+} (T = 13.4K). Solid line is calculated from $P(\alpha) = 0.14\ cos2\alpha$.

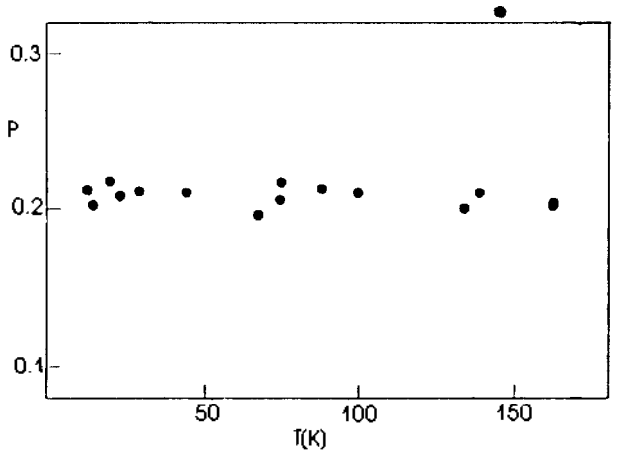

Figure 5. Temperature dependence of polarization of the 354 nm emission from RbCl:Pb^{2+}.

the same temperature. As shown in Figure 3, the polarization of the A-band emission is nearly independent of the excitation energy. The degree of polarization is positive over the whole A-band absorption. It indicates that the excitation is mainly due to linear oscillator processes. Figure 4 shows the diagram of the polarization ratio of the A_x emission from RbCl:Pb^{2+}. When the exciting light is polarized at $\alpha = 0$ or 180°, the polarization ratio is a maximum, and at $\alpha = 90°$ it is a minimum. At $\alpha = 45$ or 135°, the polarization ratio changes from positive to negative (or *vice versa*). Significantly, the absolute value of the polarization ratio at $\alpha = 90°$ is close to the value at $\alpha = 0$ or 180°. The dependence of polarization of the A_x emission on temperature was also investigated, with the exciting light polarized at $\alpha = 180°$. As shown in Figure 5, the degree of polarization is nearly independent of temperature.

Discussion

The dependence of the polarization on the angle of the exciting light suggests that the emitting dipole, corresponding

Table 1. Polarization ratio, defined by equation (2), where the unit vector of π_s, (λ_i, μ_i, ν_i) is given by: (±1, 0, 0), (0, ±1, 0) and (0, 0, ±1) for the C_4 symmetry, (±1, ±1, ±1), (±1, ±1, ∓1), (±1, ∓1, ±1) and (±1, ∓1, ∓1) for the C_3 symmetry, and (±1, 0, ±1), (0, ±1, ∓1), (±1, ∓1, 0), (±1, ±1, 0), (±1, 0, ∓1) and (0; ±1, ±1) for the C_2 symmetry.

symmetry axis of the emitting center	perpendicular (100) - (010)
C_4	$cos2\alpha$
C_3	0
C_2	$\frac{1-(2+cos^2\alpha)sin^2\alpha}{2+cos^2\alpha}$

to a Pb^{2+}-v_c^- pair, should have a preferential orientation relative to the electric vector of the exciting light. On the basis of the experimental results of the polarization spectra, the absorbing electric dipole oscillator is linear (π_s). Assuming that the absorbing and emitting oscillators are identical, we consider only three possible orientations of π_s: along the four-fold (C_4), three-fold (C_3) and two-fold (C_2) symmetry axes.

Letting the unit vector of π_s be (λ_i, μ_i, ν_i) and the electric vector of the exciting light, $\vec{E}_s$, be (l, m, n), the probability of the excitation of π_s is proportional to the mean-square value of the electric field component, given by $(l\lambda_i + m\mu_i + n\nu_i)^2$. When the excitation takes place at angle α (with respect to the z axis) along the x axis, the equation becomes $(\mu_i sin\alpha + \nu_i cos\alpha)^2$. The intensity of the emission which passes through the analyzer oriented at angle β with respect to the z axis is given by

$$I = I_0 \Sigma (\mu_i \sin\alpha + \nu_i \cos\alpha)^2 (\lambda_i \sin\beta + \nu_i \cos\beta)^2 \quad (1)$$

where I_0 depends on the experimental condition. Setting $\beta = \alpha$ for $I_{\parallel}(\alpha)$ and $\beta = \alpha + \pi/2$ for $I_{\perp}(\alpha)$, the polarization ratio at angle α is defined by:

$$P(\alpha) = \{I_{\parallel}(\alpha) - I_{\perp}(\alpha)\} / \{I_{\parallel}(\alpha) + I_{\perp}(\alpha)\} \quad (2)$$

The mathematical formulas of $P(\alpha)$ for the three orientations of π_s are listed in Table 1. Using the equations in Table 1, the orientation of the Pb^{2+}-v_c^- dipole can be deduced from the results of the polarization ratio.

The experimental results of the polarization diagram of the A-band emission from RbCl:Pb^{2+} agree well to the equation $k_d cos^2\alpha$ where k_d is a depolarization factor. The forgoing indicates that the Pb^{2+}-v_c^- dipoles have the C_4 symmetry. This symmetry would result if the cation vacancy were located at the (nnn) position with respect to the Pb^{2+} ion.

Previously[8], the temperature effect on the polarization of the A-band emission from KX:Pb^{2+} was treated in terms of the energy-level scheme and decay kinetics for the RES's. In this model[11,12], the spin-orbit interaction is taken as the zero-order approximation and the Jahn-Teller interaction with the E_g modes is regarded as a perturbation, since strong spin-orbit interaction of Pb^{2+} ion in crystal field causes the reduction in the Jahn-Teller stabilization. Mixing of $^3T_{1u}$ and $^1T_{1u}$ states due to off-diagonal elements in the spin-orbit matrix reduces the three-fold $^3T_{1u}$ state to $^3T_{1u}^*$. The reduced three-fold state is described in terms of electronic orbitals (X, Y, Z) and spin functions (x, y, z) as follows: $^3T_{1u,x}^* = (|Y_z> - |Z_y>)^*$, $^3T_{1u,y}^* = (|Z_x> - |X_z>)^*$ and $^3T_{1u,z}^* = (|X_y> - |Y_x>)^*$. When the Jahn-Teller stabilization occurs along the x axis (hereafter called case 1), T_x^* and A_1^* states are stabilized through the electronic orbital X state, while, with the Jahn-Teller axis along y (case 2) or z (case 3) axes, the two lower levels belong to (T_z^*, T_y^*), and (T_x^*, T_y^*), respectively. The v_c^- located on an axis different from the Jahn-Teller axis would split the two lower levels by a small amount (less than 1.5 meV)[11], compared to the Jahn-Teller stabilization energy. According to the APES[11], two kinds of minima (X and T*) are found to coexist on each levels. Hence, the doubly degenerate X minima exist as a stationary point and the T* minimum coexists with very shallow depth. In addition to the two lower levels, the $^3A_{1u}$ APES must be also included to account for the relaxation process involved in the A-band emission. This $^3A_{1u}$ APES is just lying below only the X minima. Exciting light polarized along the z axis causes transitions from the ground state ($^1A_{1g}$) to the T_z^* potential well and consequently, cases 1 and 2 could account for the polarization of the A-band emission. If the two lower levels of cases 1 and 2 are equally populated due to nonradiative transitions between the T_z^* and the other wells, the degree of polarization becomes 1/3.

The main effect of the thermal depolarization could be attributed to nonradiative transitions between the two lower levels and the metastable level. The probabilities of the nonradiative and the reversed nonradiative transitions are described by the Bose-Einstein distribution: $N = 1/\{exp(D_e/kT)-1\}$. Assuming that the transitions occurs *via* one phonon process, the probabilities of the nonradiative and the reversed nonradiative transitions between the two lower levels and the metastable level are proportional to $R = (1+N)$ and $R' = N$, respectively. The energy difference, D_e, between the X minima and the metastable level is indicative of the Jahn-Teller stabilization. In other words, the increase in the Jahn-Teller stabilization coupling to the E_g modes results in the decrease in the D_e magnitude. With $D_e = 57$ meV[13], R is nearly constant in the experimental temperature range and R′ is negligible. In addition, nonradiative transitions between the two kinds of minima are also negligible since the population of the upper minimum (T*) is very small, compared with that of the X minima, due to the shallow depth of the T* minimum. Consequently, the polarization of the A-band emission from KbCl:Pb^{2+} has temperature independence because of the large value of D_e.

Conclusions

When the Jahn-Teller effect is sole cause of polarization, one expects that the polarization decreases at high temperature because of the nonradiative transition between the Jahn-Teller wells and the metastable well. The persistence of polarization to high temperature for Pb^{2+} ions is due to the Pb^{2+}-v_c^- complex oriented along the C_4 symmetry axis. The temperature independence of polarization of the A-band emission from RbCl:Pb^{2+} is due to the strong spin-orbit interaction of Pb^{2+} which reduces strongly the Jahn-Teller stabilization.

Acknowledgments. The author gratefully acknowledges the Korean Science and Engineering Foundation for financial support.

References

1. P. P. Feofilov, "The Physical Basis of Polarized Emission" (authorized translation from Russian, Consultants Bureau, New York, 1961).
2. C. C. Klick and W. D. Compton, *J. Phys. Chem. Solids*, **7**, 170 (1958).
3. S. G. Zazubovich, L. E. Lushchik and Ch. B. Lushchik, *Opt. Spectrosc.*, **15**, 203 (1963).
4. A. Fukuda, S. Makishima, T. Mabuchi and R. Onaka, *J. Phys. Chem. Solids*, **28**, 1763 (1967).
5. A. Wasiela, Y. M. d'Aubigne and R. Romestain, *J. Phys. C: Solid Stat Phys.*, **13**, 3057 (1980).
6. Le Si Dang, P. W. M. Jacobs and D. J. Simkin, *J. Phys. C: Solid State Phys.*, **18**, 3567 (1985).
7. A. Scacco, P. W. M. Jacobs, T. F. Belliveau, J. G. Kang and D. J. Simkin, *J. Lumin.*, **31/32**, 145 (1984).
8. Jun-Gill Kang and David J. Simkin, submitted to *J. Lumin.* (1986).
9. Jun-Gill Kang, *Bull. Korean Chem. Soc.*, **7**, 50 (1986).
10. E. E. Bukke, N. N. Grigor'ev and M. V. Fok, "Luminescence Centers in Crystals" (Proceedings (Trudy) of the P. N. Lebedev Consultants Breau, New York and London, 1976).
11. J. G. Kang, F. Cusso, T. F. Belliveau and D. J. Simkin, *J. Phys. C: Solid Stat Phys.*, **18**, 4753 (1985).
12. Jun-Gill Kang, Chung-Gun Chang and David J. Simkin, submitted to *J. Lumin.* (1986).
13. K. Schmitt, V. S. Sivasankar and P. W. M. Jacobs, *J. Lumin.*, **27**, 313 (1982).

Studies on the Formation and Stability of Colloids(II): pH and Temperature Effects on the Secondary Micelle Formation of Sodium Deoxycholate

Joon Woo Park* and Hesson Chung

Department of Chemistry, Ewha Womans University, Seoul 120. *Received January 26, 1987*

The micelle formation of NaDC was studied by fluorometric and viscometric measurements. The thermodynamic parameters of the primary and secondary micellization of the bile salt were evaluated. The primary micelle formation was appeared to be an entropy driven process due to hydrophobic effect, while the major driving force for secondary micelle formation of the bile salt is the large negative enthalpy. The secondary micelle provides less hydrophobic environment to pyrene than the primary micelle does. The cooperative aggregation of primary micelles via hydrogen bond formation was proposed for the secondary micelle formation.

Introduction

The micellization of bile salts has been a subject of extensive investigation for a long period of time due to their unique characteristics which are closely related to the physiological and biochemical roles of bile salts[1]. The micellizing properties of bile salts depend greatly on the number of hydroxy groups attached to the parent cholanic acid. At low ionic strength, typically adjusted with NaCl, the bile salts form micelles of aggregation number of about or less than 10. Unlike trihydroxy series, the dihydroxy bile salts form large micelles at moderately increased ionic strength and bile salts concentration. D. M. Small termed the large micelle as secondary micelle to differentiate this from small (primary) micelle[1].

The formation of secondary micelles, which is maifested by increased viscosity and ultimate gelation on standing of the bile salt solutions was first reported for sodium deoxycholate(NaDC) by two independent groups in 1958[2,3]. Sodium salts of ursodeoxycholate(NaUDC) and chenodeoxycholate (NaCDC), and mixtures of these with conjugated dihydroxy bile salts also form secondary micelles, but require lower pH, and much higher bile salts and NaCl concentrations than NaDC[4-6]. The secondary micellization(gelation) of NaDC solutions is favored by low pH and high ionic strength[7]. The micelle is also stabilized as temperature is lowered[2,8], and high pressure is applied[8]. Most of investigators agreed that the secondary micelles, gel, of the bile salts are formed by aggregation of primary micelles. However, details on the mechanism of the aggregation is not known unequivocally. Sugihara et al.[8] measured the sol-gel transition of NaDC by conductometry and reported thermodynamic parameters of gelation. The critical concentration of secondary micelle formation of NaDC was also measured by Sesta et al. by densitometry and viscometry[9]. These studies were performed in the absence of NaCl. On the other hand, the light scattering[5,6] and ultrasound[10] studies on the conjugated dihydroxy bile salt did not reveal the critical concentration for the secondary micellization, but indicated that the primary micelles grow gradually above the CMC of primary micelle formation.

In this study, we examined the critical concentration of NaDC, for both primary and secondary micellization. We also investigated the effects of pH and temperature on the processes to obtain information on the mechanism of the micellization. These experiments were performed near physiological pH and ionic strength, because of the interest of the phenomena in biological fluids. The formation of primary micelle was followed by fluorometric method using pyrene as a probe[11], and the secondary micellization(gelation) was studied by viscometric measurements.